

*To be published in Journal of the Optical Society of America B:*

**Title:** Efficient Method for Analyzing Leaky Cavities in Two-dimensional Photonic Crystals

**Authors:** Ya Yan Lu and Shaojie Lu

**Accepted:** 19 October 2009

**Posted:** 21 October 2009

**Doc. ID:** 116151



# Efficient Method for Analyzing Leaky Cavities in Two-dimensional Photonic Crystals

Shaojie Li and Ya Yan Lu

*Department of Mathematics, City University of Hong Kong*

*Kowloon, Hong Kong*

Published by

An efficient numerical method is developed for analyzing leaky cavities in two-dimensional photonic crystals, assuming that the cavities are located in the vicinity of a photonic crystal waveguide or close to a homogeneous medium. A leaky cavity mode is characterized by its complex eigenfrequency, and by the outgoing wave behavior of the field in the nearby waveguide or homogeneous medium. In our method, the eigenfrequency of a leaky cavity mode is determined from a condition formulated on one single edge of a defect unit cell. Such a condition is obtained by using rigorous boundary conditions to terminate photonic crystal waveguides and homogeneous media, Dirichlet-to-Neumann maps of the unit cells to reduce the problem to the cell edges, and standard Gaussian elimination to further reduce the problem to one single edge. The reduction process can be performed efficiently. Accurate solutions can be obtained when a small number of discrete points are used on each edge of the unit cells. © 2009 Optical Society of America

*OCIS codes:* 050.5298,000.4430

## 1. Introduction

Optical cavities are important elements in photonic devices with many different applications. They are used in low threshold lasers and various nonlinear optical devices, such as wavelength converters and optical switches, since light can be confined in cavities where light-matter interactions are enhanced. Cavities are also used in many filters, since they can be used to alter the transmission of light through the resonant tunneling effect. Due to the existence of bandgaps which prohibit the propagation of light in all directions, photonic crystals (PhCs) are ideal material to design cavities. Theoretically, cavities in PhCs can be designed by modifying one or more unit cells in an otherwise perfectly periodic and infinite PhC. In practice, light has to be coupled into and out of a cavity for various applications, therefore, the cavity has to be placed near a waveguide or free space. Such a practical cavity is always a leaky cavity with a finite quality factor.

Numerical methods are essential in the analysis, design and optimization of optical cavities in PhCs. The finite-difference time-domain (FDTD) method is widely used [1–5], but it requires prohibitive computer resources even for two-dimensional (2D) problems. The accuracy of a FDTD solution can be quite limited, if the grid size is not small enough to accurately resolve the material interfaces, or if the total simulation time is not sufficiently long. To find the quality factor of a leaky cavity, it is important to have accurate outgoing radiation boundary conditions. While the perfectly matched layer (PML) technique [6] is widely used, it is in fact not effective to truncate periodic structures, such as a PhC waveguide. In principle, cavities can be solved as an eigenvalue problem of the Maxwell's equations, where the squared frequency is the eigenvalue. Unfortunately, it is also difficult to solve the

eigenvalue problem based on standard numerical methods, such as the finite difference, finite element [7] and plane wave expansion (Fourier series) [1, 8] methods. These numerical methods give rise to large matrix eigenvalue problems that are difficult to solve. Standard eigenvalue solvers such as the QR method [9] can only handle relatively small matrices. Typical iterative eigenvalue solvers, such as the ARPACK [10], are effective only for the smallest (or largest) a few eigenvalues, but cavity modes correspond to interior eigenvalues. Leaky cavity modes are more difficult, not only because they correspond to complex eigenvalues, but also because they require accurate outgoing radiation conditions for domain truncation. For dispersive media, the eigenvalue problem becomes nonlinear and more difficult to solve, since the matrix entries depend on the frequency, i.e., the eigenvalue.

In a recent paper [11], we developed an efficient method for computing ideal cavities in 2D PhCs. These cavities are local defects in an otherwise perfectly periodic and infinite PhC, therefore, their eigenfrequencies are real and the quality factor is infinite. The main idea is to reduce the eigenvalue problem on the entire 2D plane to a condition on one or a few edges of a defect unit cell, and then solve the eigenfrequency from the reduced condition iteratively. The reduction process involves two steps. The eigenvalue problem is first reduced to a condition on all edges of the unit cells in a properly truncated domain. This is achieved by using the Dirichlet-to-Neumann (DtN) maps of the unit cells. The DtN map of a unit cell is an operator that maps the wave field to its normal derivative on the cell boundary, and it can be approximated by a small matrix. The second step is actually just standard Gaussian elimination. We can eliminate all but one or a few edges of a defect unit cell, and obtain a much smaller condition for the eigenfrequency. If we use  $N$  points to discretize each edge, the condition on one single edge is that an  $N \times N$  matrix (depending on the frequency) must

be singular. Typically,  $N$  is around 10.

In this paper, we extend the DtN map method to leaky cavities in 2D PhCs, where the cavities are located near a PhC waveguide or an unbounded homogeneous medium. For the ideal cavities considered in [11], the domain can be easily truncated, because the eigenfunction decays exponentially away from the defect unit cells. For a leaky cavity placed near a PhC waveguide, the cavity mode exhibits outgoing wave behavior in the waveguide, and the magnitude of the field (in the waveguide) actually increases as the distance to the cavity increases. Therefore, the PhC waveguide cannot be truncated with simple boundary conditions. Our approach is to apply a rigorous boundary condition that terminates the PhC waveguide. Such a condition was derived in [12] for propagation problems in PhC devices at a real frequency. We modify the condition for complex frequencies corresponding to leaky cavities. We also consider the case where a cavity is near a homogeneous half-plane. In that case, we impose a rigorous boundary conditions that terminates the homogeneous medium.

## 2. The DtN map method

For 2D problems where the refractive index is invariant in the  $z$  direction and light waves propagate in the  $xy$  plane, the governing equation is

$$\rho \frac{\partial}{\partial x} \left( \frac{1}{\rho} \frac{\partial u}{\partial x} \right) + \rho \frac{\partial}{\partial y} \left( \frac{1}{\rho} \frac{\partial u}{\partial y} \right) + k_0^2 n^2 u = 0, \quad (1)$$

where  $u$  is the  $z$  component of the electric or magnetic field,  $n = n(x, y)$  is the refractive index function,  $k_0 = \omega/c$  is the free space wavenumber,  $\omega$  is the angular frequency (the time dependence is  $e^{-i\omega t}$ ),  $c$  is the speed of light in vacuum,  $\rho = 1$  or  $\rho = n^2$  for the  $E$  or  $H$  polarizations, respectively. A cavity mode is a special solution of the homogeneous Helmholtz equation (1) satisfying suitable boundary conditions at infinity. This is an eigenvalue problem

where  $k_0^2$  (or  $\omega^2$ ) is the eigenvalue and  $u$  is the eigenfunction. An ideal cavity can be created by introducing local defects in an infinite PhC. In that case, its eigenfrequency is real and is within a bandgap of the PhC. Therefore, the boundary condition is  $u \rightarrow 0$  as  $|\mathbf{x}| \rightarrow \infty$ , where  $\mathbf{x} = (x, y)$ .

We consider leaky cavities in PhCs. Two examples are shown in Fig. 1. In the first example, the cavity is placed in the vicinity of a PhC waveguide. In that case, the cavity mode behaves like outgoing Bloch waves in the waveguide (to both directions along the waveguide axis), but its magnitude actually increases as the distance to the cavity increases and blows up at infinity. The second example is a cavity in a PhC that occupies the left half-plane, while the other half-plane is a homogeneous medium. Since we assume that the real part of the eigenfrequency is within a bandgap of the bulk PhC, the cavity mode decays exponentially to zero as  $|\mathbf{x}| \rightarrow \infty$  if  $x < 0$ . In the right half-plane, the mode acts like the field radiated from a source, but its magnitude also increases as  $|\mathbf{x}| \rightarrow \infty$ . To simulate the leaky cavities, it is crucial to set up accurate outgoing radiation conditions for nearby waveguides and homogeneous media. The PML technique works well in homogeneous media, but fails in PhC waveguides. In a homogeneous medium, a PML turns an outgoing wave and an incoming wave to an exponentially decaying and exponentially growing field, respectively. This allows us to obtain mostly outgoing waves when the PML is truncated with a simple zero boundary conditions. Unfortunately, a PML cannot separate outgoing and incoming Bloch waves. Therefore, it cannot be used to simulate the outgoing radiation condition in a PhC waveguide.

Our approach is to use rigorous boundary conditions to terminate PhC waveguides and homogeneous media. For the two examples concerned, we truncate the domain to the rect-

angles shown in Fig. 1. For the cavity near a PhC waveguide, the truncated domain  $S$  covers only one unit cell in the horizontal direction which we assume is given by  $0 < x < a$ , where  $a$  is the lattice constant of the bulk PhC. On the top and bottom edges of  $\partial S$  (the boundary of  $S$ ), we use the zero Dirichlet boundary condition, i.e.,  $u = 0$ , since the field decays exponentially in the PhC. On the two vertical edges of  $\partial S$  at  $x = 0$  and  $x = a$ , we impose the following boundary conditions

$$\frac{\partial u}{\partial x} = \mathcal{L}^- u, \quad x = 0, \quad (2)$$

$$\frac{\partial u}{\partial x} = \mathcal{L}^+ u, \quad x = a, \quad (3)$$

where  $\mathcal{L}^+$  and  $\mathcal{L}^-$  are two operators acting on functions of  $y$ . These two operators depend on the unknown frequency  $\omega$  and they are approximated by matrices when  $y$  is discretized. We describe their definitions and matrix approximations in Section 3. For the cavity near the homogeneous half plane, the truncated domain  $S$  covers more unit cells. On the right edge of  $\partial S$ , i.e.,  $x = 0$ , we use the following boundary condition:

$$\frac{\partial u}{\partial x} = \mathcal{B} u, \quad x = 0, \quad (4)$$

where  $\mathcal{B}$  is an operator acting on functions of  $y$ . On the other three edges of  $\partial S$ , we use the simple condition  $u = 0$ . The details about operator  $\mathcal{B}$  and its approximations are given in Section 4.

Once the boundary conditions for terminating PhC waveguides and homogeneous media are established, the remaining steps are identical to those given in [11]. First, we divide the truncated domain  $S$  into unit cells and calculate their DtN maps. For both examples, we have square unit cells as shown in Fig. 1. Notice that the unit cells are either regular

ones involving a circular cylinder or defect ones of a homogeneous medium. We only need to calculate the DtN maps for the two different kinds of unit cells. Let  $\Omega$  be a unit cell, the DtN map is the operator  $\Lambda$  satisfying

$$\Lambda u = \frac{\partial u}{\partial \nu} \quad \text{on} \quad \partial\Omega, \quad (5)$$

where  $u$  is an arbitrary solution of (1),  $\partial\Omega$  is the boundary of  $\Omega$  and  $\nu$  is a unit normal vector of  $\partial\Omega$ . In practice, we approximate  $\Lambda$  by a small matrix using the methods described in [13–16]. For a square unit cell, if each edge of  $\partial\Omega$  is discretized by  $N$  points, then  $\Lambda$  is approximated by a  $(4N) \times (4N)$  matrix. Typically, the  $N$  points on each edge are chosen uniformly and the corners of  $\Omega$  are avoided.

Next, we set up a system of equations for  $u$  on all edges of unit cells in the truncated domain  $S$ . Based on the DtN maps of the unit cells, we can write down one equation for each edge by matching the normal derivative of  $u$  (or  $\rho^{-1}\partial_\nu u$  if the edge is a physical interface and the  $H$  polarization is being studied). For an interior edge in the truncated domain, we calculate  $\partial_\nu u$  using the DtN maps of the two neighboring unit cells. This leads to an equation connecting all edges in these two unit cells. On a boundary edge, we match  $\partial_\nu u$  using the DtN map of one unit cell and the exact boundary condition like (2), (3) or (4). When all these equations are put together, we obtain

$$A(\omega)U = 0, \quad (6)$$

where  $U$  is a column vector for  $u$  on all edges in the truncated domain  $S$  and  $A$  is a square matrix that depends on  $\omega$ . If the total number of edges is  $M$ , then the length of  $U$  is  $NM$  and the size of  $A$  is  $(NM) \times (NM)$ . Notice that  $A$  is a sparse matrix, since each equation

for an interior edge is only related to the small number of edges in the two neighboring unit cells.

Finally, we reduce Eq. (6) to a condition on one single edge and solve the eigenfrequency of the cavity mode. In principle, we can find the frequency from the condition that the matrix  $A(\omega)$  is singular. Since the size of  $A$  is relatively large, this approach is still expensive. Based on standard Gaussian elimination, we can reduce (6) to

$$B(\omega) u_* = 0, \quad (7)$$

where  $u_*$  is the wave field on a particular edge, usually an edge of the defect unit cell on which the field is expected to be strong. For the two examples in Fig. 1, the edge for  $u_*$  is shown as the solid line inside the truncated domain  $S$ . For the eigenfrequency of the cavity mode, the matrix  $B(\omega)$  should be singular. Therefore, we can solve  $\omega$  from

$$\lambda_1(B(\omega)) = 0 \quad \text{or} \quad s_1(B(\omega)) = 0 \quad (8)$$

iteratively, where  $\lambda_1$  is the smallest eigenvalue (in absolute value) and  $s_1$  is the smallest singular value of  $B(\omega)$ .

### 3. Boundary conditions for PhC waveguides

For a real frequency, a rigorous boundary condition for terminating a PhC waveguide was established in [12]. In this section, we discuss the necessary modifications for complex frequencies of leaky cavity modes. The boundary condition in [12] was derived using Bloch modes of the PhC waveguide and an operator  $\mathcal{M}$  characterizing one period of the waveguide. Let us consider the example shown in Fig. 1(a) and concentrate on the semi-infinite PhC waveguide to the right of the vertical line at  $x = a$ . For one period of this waveguide

given by  $x_j < x < x_{j+1}$  where  $x_j = ja$  and  $j \geq 1$ , we can find an operator  $\mathcal{M}$  such that

$$\mathcal{M} \begin{bmatrix} u_j \\ u_{j+1} \end{bmatrix} = \begin{bmatrix} \mathcal{M}_{11} & \mathcal{M}_{12} \\ \mathcal{M}_{21} & \mathcal{M}_{22} \end{bmatrix} \begin{bmatrix} u_j \\ u_{j+1} \end{bmatrix} = \begin{bmatrix} \partial_x u_j \\ \partial_x u_{j+1} \end{bmatrix}, \quad (9)$$

where  $u_j$  and  $\partial_x u_j$  denote  $u$  and  $\partial_x u$  evaluated at  $x_j$ , etc. The operator  $\mathcal{M}$  is also given in  $2 \times 2$  block form. Consistent with the truncated domain  $S$ , we assume that  $y$  in the semi-infinite PhC waveguide is also truncated. Assuming that the interval of  $y$  covers  $m$  unit cells and each edge of the unit cells is discretized by  $N$  points, then  $u_j$  is approximated by a column vector of length  $mN$ ,  $\mathcal{M}$  is approximated by a  $(2mN) \times (2mN)$  matrix, etc. As shown in [17],  $\mathcal{M}$  can be easily obtained by merging the DtN maps of the unit cells in one period of the waveguide.

Based on the operator  $\mathcal{M}$ , we can calculate the Bloch modes of the PhC waveguide [17]. In a waveguide which is periodic in  $x$ , a Bloch mode is a special solution of Eq. (1) given as  $\phi(x, z) = \Phi(x, z)e^{i\alpha x}$ , where  $\Phi$  is also periodic in  $x$  and  $\alpha$  is a constant. The Bloch modes can be solved from the following eigenvalue problem [17]:

$$\begin{bmatrix} \mathcal{M}_{11} & -I \\ \mathcal{M}_{21} & 0 \end{bmatrix} \begin{bmatrix} \phi \\ \partial_x \phi \end{bmatrix} = \mu \begin{bmatrix} -\mathcal{M}_{12} & 0 \\ -\mathcal{M}_{22} & I \end{bmatrix} \begin{bmatrix} \phi \\ \partial_x \phi \end{bmatrix}, \quad (10)$$

where  $\mu = e^{i\alpha a}$  is the eigenvalue,  $\phi$  and  $\partial_x \phi$  are evaluated at  $x_j$ , and  $I$  is the identity operator (matrix in the discrete case). Using the Bloch modes, we can expand the wave field of the cavity mode in the PhC waveguide as

$$u(x, y) = \sum_k c_k \Phi_k(x, z) e^{i\alpha_k x}, \quad x > a. \quad (11)$$

Actually, the Bloch modes appear in pairs, namely, if  $\mu$  is an eigenvalue of (10), then so is  $1/\mu$ . However, the sum in (11) should include only  $mN$  Bloch modes among the total of  $2mN$  modes of (10). For the case when  $\omega$  is real [12], we choose the eigenvalues such that either

$|\mu| < 1$  or  $|\mu| = 1$  (i.e.  $\alpha$  is real) and the average power flux on the vertical line at  $x_j$  is positive. This ensures that the Bloch mode expansion (11) includes only propagating modes that propagate towards  $x = +\infty$  and evanescent modes that decay as  $x$  is increased. When the frequency  $\omega$  is complex, the condition  $|\mu| \leq 1$  is not always valid, since an originally outgoing propagating Bloch mode (when  $\omega$  is real) can now grow as  $x$  is increased. Our approach is to select the Bloch modes based on their continuous dependence on the imaginary part of  $\omega$ . First, we calculate and select the Bloch modes using the real part of  $\omega$  as the frequency. For the complex  $\omega$ , we require that the eigenvalues of the Bloch modes are close to those selected eigenvalues for the real frequency. The method works since the imaginary part of the complex frequency  $\omega$  of a leaky cavity is typically very small.

Based on the Bloch mode expansion (11), we can define a linear operator  $\mathcal{T}$  satisfying

$$\mathcal{T}\phi_k = \mu_k\phi_k, \quad k = 1, 2, \dots \quad (12)$$

where  $\phi_k$  is the  $k$ th Bloch mode evaluated at  $x_j$ . Since  $\mathcal{T}$  is linear, we have  $\mathcal{T}u_j = u_{j+1}$ , therefore, from the second equation of (9), we obtain

$$\partial_z u_j = \mathcal{L}^+ u_j \quad \text{for} \quad \mathcal{L}^+ = \mathcal{M}_{11} + \mathcal{M}_{12}\mathcal{T}. \quad (13)$$

The above  $\mathcal{L}^+$  is the operator used in the boundary condition (3). The operator  $\mathcal{L}^-$  used in (2) can be similarly derived. If one period of the PhC waveguide given by  $x_j < x < x_{j+1}$ , has a mirror symmetry with respect to its center at  $(x_j + x_{j+1})/2$ , then  $\mathcal{L}^- = -\mathcal{L}^+$ .

#### 4. Boundary condition for homogeneous media

For the example shown in Fig. 1(b), a PhC with a cavity is given in the left half plane ( $x < 0$ ) and a lossless homogeneous medium is given in the right half plane ( $x > 0$ ). In

the following, we describe a rigorous boundary condition on the line at  $x = 0$  for complex frequencies corresponding to leaky cavity modes.

For a real frequency, we can write down the general outgoing radiating field in the right half-plane through a Fourier transform in the  $y$  direction. If the Fourier transform of  $u(0, y)$  is

$$u(0, y) = \int_{-\infty}^{\infty} \hat{u}(\beta) e^{i\beta y} d\beta, \quad (14)$$

then the field in the right half-plane is

$$u(x, y) = \int_{-\infty}^{\infty} \hat{u}(\beta) e^{i(\alpha x + \beta y)} d\beta, \quad x > 0, \quad (15)$$

where  $\alpha = \sqrt{k_0^2 n_0^2 - \beta^2}$  and  $n_0$  is the refractive index for  $x > 0$ . The standard square root of a complex number  $z$  is defined as  $\sqrt{z} = \sqrt{|z|} e^{i\theta/2}$  if  $z = |z| e^{i\theta}$  for  $-\pi < \theta \leq \pi$ , and it is used to calculate  $\alpha$ . Therefore,  $\alpha$  is real and positive if  $k_0^2 n_0^2 > \beta^2$ , and  $\alpha$  is pure imaginary with a positive imaginary part if  $k_0^2 n_0^2 < \beta^2$ . This implies that  $u$  given in (15) is a superposition of propagating plane waves that propagate towards  $x = +\infty$  and evanescent plane waves that decay exponentially as  $x$  is increased. Notice that the negative real axis is the branch cut of the standard square root function. Since our assumed time dependence is  $e^{-i\omega t}$ , the imaginary part of the complex frequency  $\omega$  of a leaky cavity mode must be negative. This means that  $k_0^2 n_0^2 - \beta^2$  is slightly below the real axis. In particular, if  $k_0^2 n_0^2 - \beta^2$  is close to a large negative real number, the standard square root will give an  $\alpha$  that has a negative imaginary part. This exponentially growing solution is incorrect, since it disconnects with the exponential decaying solution when  $\omega$  is real. A simple way to obtain the correct  $\alpha$  is to modify the definition of the square root function, so that the branch cut is along the negative

imaginary axis, that is

$$\sqrt{z} = \sqrt{|z|}e^{i\theta/2}, \quad \text{if } z = |z|e^{i\theta} \quad \text{for } -\frac{\pi}{2} < \theta \leq \frac{3\pi}{2}. \quad (16)$$

When the above square root function is applied to calculate  $\alpha$ ,  $u$  given in (15) is the correct outgoing radiating field corresponding to the complex frequency. From (15), we can find  $\partial_x u$  and evaluate it at  $x = 0$ , i.e.,

$$\partial_x u(0, y) = \int_{-\infty}^{\infty} i\alpha \hat{u}(\beta) e^{i\beta y} d\beta. \quad (17)$$

Therefore, we can write the boundary condition as  $\partial_x u = \mathcal{B}u$  at  $x = 0$ , if we define an operator  $\mathcal{B}$  such that  $\mathcal{B}f = g$ , where

$$f(y) = \int_{-\infty}^{\infty} \hat{f}(\beta) e^{i\beta y} dy, \quad g(y) = \int_{-\infty}^{\infty} i\alpha \hat{f}(\beta) e^{i\beta y} dy.$$

However, the definition of  $\mathcal{B}$  based on Fourier transform is not convenient for practical numerical implementation. It is much easier to approximate  $\mathcal{B}$  based on truncating  $y$  using perfectly matched layers [6]. Consistent with the truncated domain  $S$  described in Section 2, we assume that  $y$  is truncated to  $-d < y < d$ . PMLs are needed near  $y = \pm d$  to model radiation fields that propagate to  $y = \pm\infty$ . Based on the complex coordinate stretching formulation, a PML corresponds to replacing  $y$  in the Helmholtz equation by  $\hat{y} = y + i \int_0^y \sigma(\tau) d\tau$ , where  $\sigma(y) = 0$  for  $|y| \leq h$  and  $\sigma(y) > 0$  for  $|y| > h$ , and  $y = \pm h$  are the boundaries of the PMLs. For  $x > 0$ , the Helmholtz equation becomes

$$\partial_{\hat{y}}^2 u + \partial_x^2 u + k_0^2 n_0^2 u = 0$$

and the boundary condition is  $u = 0$  at  $y = \pm d$  (i.e.,  $\hat{y} = \pm \hat{d}$ ), where  $\hat{d} = d + i \int_0^d \sigma(\tau) d\tau$ .

This allows us to write down the general solution in the right half-plane as

$$u(x, y) = \sum_{k=1}^{\infty} c_k e^{i\alpha_k x} \sin[\beta_k(\hat{y} + \hat{d})] \quad (18)$$

where

$$\beta_k = k\pi/(2\hat{d}), \quad \alpha_k = \sqrt{k_0^2 n_0^2 - \beta_k^2}. \quad (19)$$

In the above,  $\alpha_k$  is calculated by the modified square root function given in (16). If we define  $\mathcal{B}$  as a linear operator satisfying

$$\mathcal{B} \sin[\beta_k(\hat{y} + \hat{d})] = i\alpha_k \sin[\beta_k(\hat{y} + \hat{d})], \quad k = 1, 2, \dots \quad (20)$$

then it is easy to verify that  $u$  given in (18) satisfies the boundary condition (4) at  $x = 0$ .

In the fully discretized case,  $y$  is truncated to cover  $m$  unit cells (i.e.  $2d = ma$ ) and it is discretized by  $mN$  points, then the operator  $\mathcal{B}$  is approximated by an  $(mN) \times (mN)$  matrix. From (20), we know that the eigenvalues and eigenvectors of the matrix  $\mathcal{B}$  are  $i\alpha_k$  and  $\sin[\beta_k(\hat{y} + \hat{d})]$  evaluated at the  $mN$  points of  $y$ , for  $1 \leq k \leq mN$ .

## 5. Numerical examples

In this section, we demonstrate our method by a few numerical examples. For all these examples, we consider the  $E$  polarization and use the same background PhC, namely, a square lattice of dielectric cylinders surrounded by air, where the refractive index and the radius of the cylinders are  $n = 3.4$  and  $r = 0.2L$ , respectively. Cavities and waveguides are standard point and line defects created by removing one or a row of cylinders, respectively.

First, we consider the two examples shown in Fig. 1, where the truncated domains are also illustrated. For the cavity near a PhC waveguide, the truncated domain  $S$  covers 15 unit cells including five regular unit cells above the defect in the positive  $y$  direction. For the cavity near a homogeneous half-plane, the defect unit cell is surrounded by six layers of regular unit cells in the positive and negative  $y$  directions, but the top and bottom layers

are being used by PMLs where the solutions are no longer physical. Using  $N = 11$  points on each edge of the unit cells, we obtain the eigenfrequency  $\omega L/(2\pi c) = 0.38003 - 0.0009074i$  for the cavity near a waveguide, and  $\omega L/(2\pi c) = 0.37868 - 0.002220i$  for the cavity near a homogeneous half-plane. The corresponding quality factors are  $Q \approx 209.4$  and  $Q \approx 85.29$ , respectively. The electric field patterns of these two leaky modes are shown in Fig. 2.

Three more examples are illustrated in Fig. 3. The first two examples are cavities in the core of a PhC waveguide, where the cavities are blocked by one or two cylinders in each side along the waveguide axis. As shown in Fig. 3, the truncated domains cover 11 unit cells in the  $y$  direction and 3 or 5 unit cells in the  $x$  direction. With  $N = 11$  points on each edge of the unit cells, the eigenfrequencies of the leaky modes are calculated as  $\omega L/(2\pi c) = 0.37696 - 0.004135i$  and  $\omega L/(2\pi c) = 0.37793 - 0.0004044i$ , for the cavities blocked by one or two cylinders, respectively. The quality factors of the these two leaky modes are  $Q \approx 45.58$  and  $Q \approx 467.3$ , respectively. The corresponding electric field patterns of the leaky modes are shown in Fig. 4. For the cavity blocked by one cylinder, it is easy to observe that the magnitude of the field in the waveguide increases as the distance to the cavity is increased. This is also true for the other examples, but it is difficult to notice when the imaginary part of the complex eigenfrequency is very small.

The third example shown in Fig. 3 is the channel-drop filter proposed in [18]. The structure involves two waveguides that are parallel to each other and two cavities located between the waveguides. The truncated domain  $S$  is also shown in Fig. 3 and it covers 6 unit cells in the  $x$  direction and 15 unit cells in the  $y$  direction. To establish rigorous boundary conditions on the vertical edges of  $\partial S$  (boundary of  $S$ ), we treat the structure with two parallel waveguides as a super-waveguide with two cores. The super-waveguide has two propagating modes with

nearly equal propagation constants. Meanwhile, the two cavities are also regarded as a super-cavity with two defect unit cells. The super-cavity supports two leaky modes which are even or odd with respect to a vertical line at the middle of the two defect cells. Using the method developed in previous sections and  $N = 11$ , we obtain the complex frequencies of these two modes. They are  $\omega L/(2\pi c) = 0.37872 - 0.0001914i$  for the odd mode and  $\omega L/(2\pi c) = 0.37831 - 0.0000546i$  for the even mode. The corresponding quality factors are  $Q \approx 989.3$  and  $Q \approx 3464$ , respectively. The electric field patterns of these two modes are shown in Fig. 5.

The eigenfrequencies reported above include 5 and 7 correct digits (including the zeros after the decimal point) for the real and imaginary parts, respectively. They are validated by increasing  $N$  (the number of points used on each edge) and enlarging the truncated domain  $S$ . For  $N = 11$ , the field in each unit cell is approximated by  $4 \times N = 44$  cylindrical waves, since the DtN maps of the unit cells are constructed using cylindrical wave expansions [13]. It is possible to get reasonable results for a much smaller  $N$ . For  $N = 5$ , the number of correct digits are roughly reduced to 3 and 5 for the real and imaginary parts, respectively. Since the real part of the complex eigenfrequency is in a bandgap of the background PhC, the results change very little when the truncated domains are further enlarged. The eigenfrequencies are solved from Eq. (8) using the Müller's method. Typically, only 3 or 4 iterations are needed to obtain a convergent result.

## 6. Conclusion

In this paper, we developed an efficient numerical method for analyzing leaky cavities in 2D PhCs, where the cavities are close to PhC waveguides or unbounded homogeneous media.

Existing numerical methods for leaky cavities are not very efficient when outgoing radiations in PhC waveguides must be simulated. Our method is an extension of our previous work [11] for ideal (non-leaky) cavities in an infinite 2D PhC background. Based on rigorous boundary conditions for terminating PhC waveguides and homogeneous media, we are able to accurately analyze leaky cavities in small truncated domains. The eigenfrequency of a leaky mode is solved iteratively from a condition on one single edge of a defect unit cell. The condition can be efficiently calculated using the DtN maps of the unit cells.

Our method is currently limited to 2D structures that are invariant in the third direction. This excludes the important case for cavities in a PhC slab. Although the method is presented for PhCs given as square lattices of cylinders, it can be easily extended to triangular lattices.

### Acknowledgments

This research was partially supported by a grant from City University of Hong Kong (Project No. 7002467).

### References

1. R. R. Villeneuve, S. H. Fan, and J. D. Joannopoulos, “Microcavities in photonic crystals: Mode symmetry, tunability, and coupling efficiency,” *Phys. Rev. B* **54**, 7837-7842 (1996).
2. K. Sakoda and H. Shiroma, “Numerical method for localized defect modes in photonic lattices,” *Phys. Rev. B* **56**, 4830-4835 (1997).
3. V. Kuzmiak and A. A. Maradudin, “Localized defect modes in a two-dimensional triangular photonic crystal,” *Phys. Rev. B* **57**, 15242-15250 (1998).

4. N. Stojić, J. Glimm, Y. Deng, and J. W. Haus, “Transverse magnetic defect modes in two-dimensional triangular-lattice photonic crystals,” *Phys. Rev. E* **64**, 056614 (2001).
5. S. P. Guo and S. Albin, “Numerical techniques for excitation and analysis of defect modes in photonic crystals,” *Opt. Express* **11**, 1080-1089 (2003).
6. J. P. Berenger, “A perfectly matched layer for the absorption of electromagnetic waves,” *J. Comput. Phys.* **114**, 185-200 (1994).
7. V. F. Rodríguez-Esquerre, M. Koshiba, and H. E. Hernández-Figueroa, “Finite-element analysis of photonic crystal cavities: Time and frequency domains,” *J. Lightwave Technol.* **23**, 1514-1521 (2005).
8. X. P. Feng and Y. Arakawa, “Defect modes in two-dimensional triangular photonic crystals,” *Japanese Journal of Applied Physics* **36**, L120-L123 (1997).
9. Z. Bai, J. Demmel, J. Dongarra, A. Ruhe, and H. van der Vorst, ed., *Templates for the Solution of Algebraic Eigenvalue Problems* (Society of Industrial and Applied Mathematics, Philadelphia, 2000).
10. R. B. Lehoucq, D. C. Sorensen, and C. Yang, *ARPACK Users’s Guide: Solution of Large-Scale Eigenvalue Problems with Implicitly Restarted Arnoldi Method* (Society of Industrial and Applied Mathematics, Philadelphia, 1998).
11. S. Li and Y. Y. Lu, “Computing photonic crystal defect modes by Dirichlet-to-Neumann maps,” *Opt. Express* **15**, 14454-14466 (2007).
12. Z. Hu and Y. Y. Lu, “Efficient analysis of photonic crystal devices by Dirichlet-to-Neumann maps,” *Opt. Express* **16**, 17383-17399 (2008).
13. Y. Huang and Y. Y. Lu, “Scattering from periodic arrays of cylinders by Dirichlet-to-

- Neumann maps,” *J. Lightwave Technol.* **24**, 3448-3453 (2006).
14. S. Li and Y. Y. Lu, “Multipole Dirichlet-to-Neumann map method for photonic crystals with complex unit cells,” *J. Opt. Soc. Am. A* **24**, 2438-2442 (2007).
  15. J. Yuan, Y. Y. Lu, and X. Antoine, “Modeling photonic crystals by boundary integral equations and Dirichlet-to-Neumann maps,” *J. Comput. Phys.* **227**, 4617-3629 (2008).
  16. H. Xie and Y. Y. Lu, “Modeling two-dimensional anisotropic photonic crystals by Dirichlet-to-Neumann maps,” *J. Opt. Soc. Am. B* **26**, 1606-1614 (2009).
  17. Y. Huang, Y. Y. Lu and S. Li, “Analyzing photonic crystal waveguides by Dirichlet-to-Neumann maps,” *J. Opt. Soc. Am. B* **24**, 2860-2867 (2007).
  18. S. Fan, P. R. Villeneuve, J. D. Joannopoulos, and H. A. Haus, “Channel drop tunneling through localized states,” *Phys. Rev. Lett.* **80**, 960-963 (1998).

## List of Figures

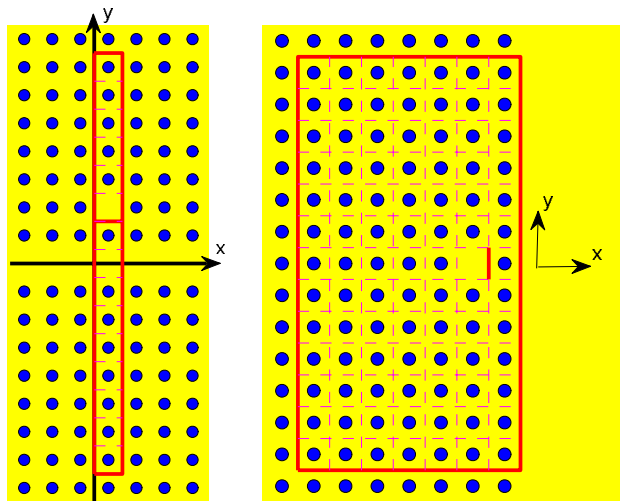
Fig. 1 (a): a cavity in the vicinity of a PhC waveguide. (b): a cavity near a homogeneous half-plane.

Fig. 2 Electric field patterns of the leaky modes in cavities near a photonic crystal waveguide (a) or a homogeneous half-plane (b).

Fig. 3 (a) and (b): cavities in the core of a photonic crystals waveguide. (c): two cavities between two photonic crystal waveguides.

Fig. 4 Electric field patterns of the leaky modes for cavities blocked by one cylinder (a) and two cylinders (b).

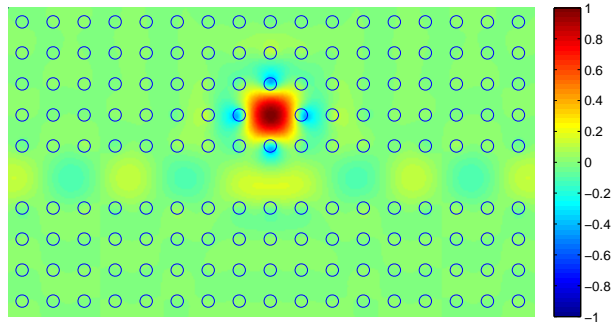
Fig. 5 Electric field patterns of the odd (a) and even (b) leaky modes for the channel-drop filter.



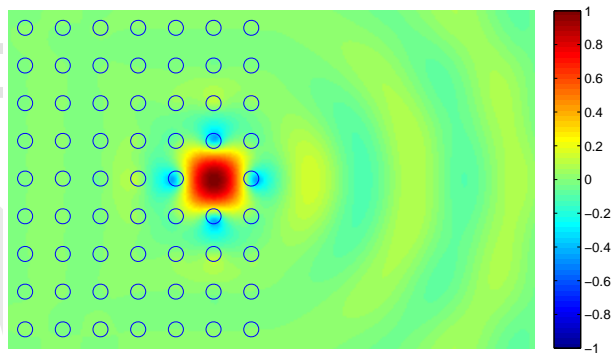
(a)

(b)

Fig. 1. (a): a cavity in the vicinity of a PhC waveguide. (b): a cavity near a homogeneous half-plane.



(a)



(b)

Fig. 2. Electric field patterns of the leaky modes in cavities near a photonic crystal waveguide (a) or a homogeneous half-plane (b).

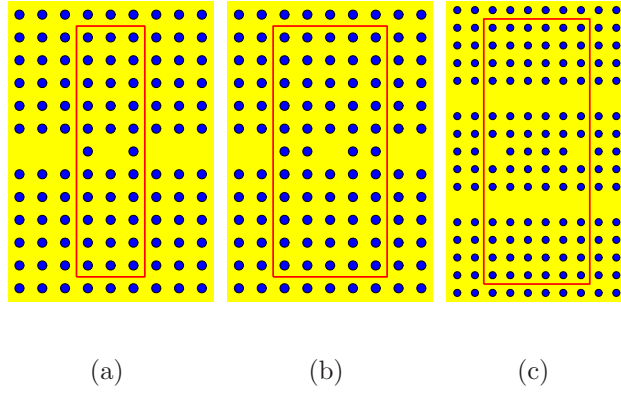
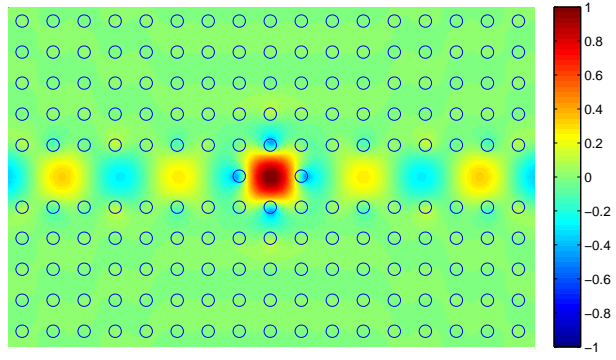
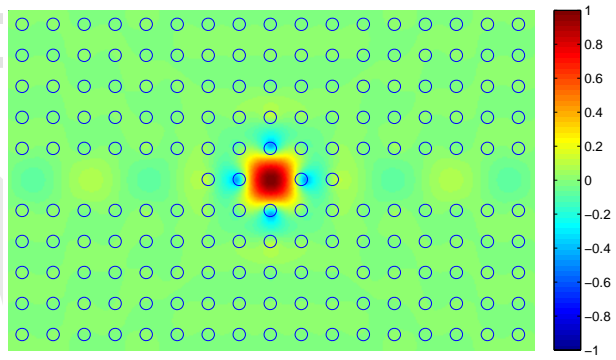


Fig. 3. (a) and (b): cavities in the core of a photonic crystals waveguide. (c): two cavities between two photonic crystal waveguides.

Published by  
OSA

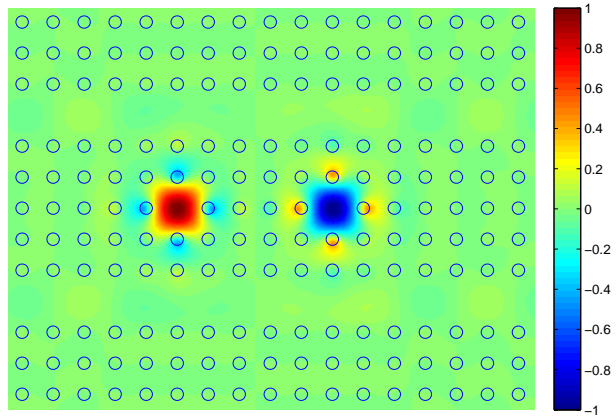


(a)

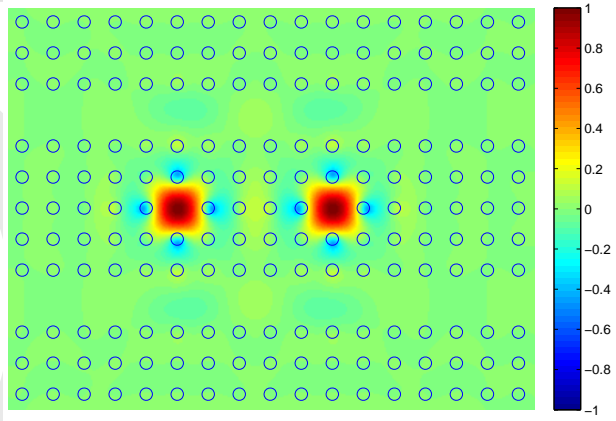


(b)

Fig. 4. Electric field patterns of the leaky modes for cavities blocked by one cylinder (a) and two cylinders (b).



(a)



(b)

Fig. 5. Electric field patterns of the odd (a) and even (b) leaky modes for the channel-drop filter.